ResearchGate

See discussions, stats, and author profiles for this publication at: https://www.researchgate.net/publication/337525932

Topological Semantics for Lumped Parameter Systems Modeling

Conference Paper · August 2019

DOI: 10.1115/DETC2019-98181

CITATIONS

0

2 authors, including:

Randi Wang

Palo Alto Research Center

4 PUBLICATIONS **1** CITATION

SEE PROFILE

All content following this page was uploaded by Randi Wang on 17 September 2022.

The user has requested enhancement of the downloaded file.

Proceedings of the ASME 2019
International Design Engineering Technical Conferences
and Computers and Information in Engineering Conference
IDETC/CIE 2019
August 18-21, 2019, Anaheim, CA, USA

IDETC2019-98181

TOPOLOGICAL SEMANTICS FOR LUMPED PARAMETER SYSTEMS MODELING

Randi Wang
Spatial Automation Laboratory
University of Wisconsin - Madison
Madison, WI 53706
Email: randi.wang@wisc.edu

Vadim Shapiro*
Spatial Automation Laboratory
University of Wisconsin - Madison
Madison, WI 53706
Email: vshapiro@wisc.edu

ABSTRACT

Behaviors of many engineering systems are described by lumped parameter models that encapsulate the spatially distributed nature of the system into networks of lumped elements; the dynamics of such a network is governed by a system of ordinary differential and algebraic equations. Languages and simulation tools for modeling such systems differ in syntax, informal semantics, and in the methods by which such systems of equations are generated and simulated, leading to numerous interoperability challenges.

We propose to unify semantics of all such systems using standard notions from algebraic topology. In particular, Tonti diagrams classify all physical theories in terms of physical laws (topological and constitutive) defined over a pair of dual cochain complexes and may be used to describe different types of lumped parameter systems. We show that all possible methods for generating the corresponding state equations within each physical domain correspond to paths over Tonti diagrams. We further propose a generalization of Tonti diagram that captures the behavior and supports canonical generation of state equations for multi-domain lumped parameter systems. The unified semantics provides a basis for greater interoperability in systems modeling, supporting automated translation, integration, reuse, and numerical simulation of models created in different authoring systems and applications. Notably, the proposed algebraic topological semantics is also compatible with spatially and temporally distributed models that are at the core of modern CAD and CAE systems.

1 INTRODUCTION

1.1 Motivation

Lumped parameter models are commonly used to describe behaviors of many engineering systems [1]. In such systems, spatially and temporally distributed physical phenomena are approximated by a finite network of abstract components that store, dissipate, or transform energy; the phenomena-specific constitutive properties of the components (e.g. generalized impedances) are estimated by domain integrals from the actual system by a process of "reticulation" [2]. Bond graphs [2], linear graphs [3], Modelica [4] and Simulink/Simscape [5] are commonly used physical modeling languages for creating, editing, and simulating lumped parameter models. These languages may differ widely in their syntax, but have similar (though not identical) semantics that specifies interconnectivity and constitutive relations of individual components in a system; the resulting model of a system created in such languages is then compiled into a system of state equations, a set of ordinary differential equations (ODEs) or differential algebraic equations (DAEs), that may be numerically solved to simulate the system's dynamic response.

Generally speaking, all modeling languages can handle the same broad class of problems but with non-trivial differences in system types, representations, state equation derivation and simulation mechanisms [3, 6, 7]. These differences in syntax and semantics of system modeling languages lead to challenges in exchange, translation, and composition of models created in these

*Address all correspondence to this author.

© 2019 by ASME

languages. Such interoperability difficulties are only likely to increase due to ubiquitous and growing adoption of physical modeling languages by industry and standards organizations.

Conceptually, there are two possible approaches to dealing with semantic interoperability issues: "point-to-point" correspondence[1] between models created in different languages, or standardization on a single neutral format that can be translated to/from models in any such languages. The first approach is more practical but is problematic because it requires $O(n^2)$ such translators, which is not only expensive, but discourages development of new languages and simulation solutions. The second approach is similar in spirit to STEP for product models, which requires the neutral format to be formally defined and include the superset of models present in any such language. These difficulties can be observed in a recent effort to extend System Modeling Language (SysML) with packages for direct communication with multiple simulation tools [8]. Recently proposed Functional Mockup Interface (FMI) [9] attempts to sidestep the semantic interoperability issues by supporting model exchange and integration via standardized XML and C-code interfaces; this approach simply shifts the responsibility for semantic correctness of these tasks to the authoring systems and users.

Irrespectively of the selected approach, semantic interoperability requires establishing formal correspondence between concepts and constructs in distinct modeling languages. This is the main goal of this paper. Our approach relies on tools from algebraic topology and well known classification of physical theories developed over the years by Tonti [10], Roth [11], Branin [12], Kron [13], and others. Importantly, this classification generalizes to higher-dimensional physical models, suggesting that the proposed framework may be extended to include spatially-distributed models represented by three-dimensional solid models, partial differential equations and finite element methods.

1.2 Outline

Section 2 briefly surveys the related works. In Section 3, we summarize the well-known algebraic topological model of physical systems, which serves as the basis for Tonti diagrams that classify physical variables, laws, and theories [10]. Tonti's classification is a starting point for the unified semantics proposed in this paper. The main results of the paper are contained in Section 4 and Section 5. We conclude in Section 6 with consequences of the proposed semantic unification, discussion of practical applications and and possible extensions.

2 RELATED WORKS

Broadly speaking, interoperability subsumes the problems of exchange and integration of simulation models created in different systems. The latter often manifests itself as the need for co-simulation [14] and/or for executable semantics in system modeling tools. For example, system engineering languages, such as SysML [15] needs to integrate with simulation models in order to predict the modelled system behavior; however, each specific tool needs a different interface, as proposed in [16] for Matlab/Simulink, in [17] for Modelica, and for bond graph in [18]. An effort to overcome these challenges was recently described in [8], where a SysML extension is proposed specifically for the purpose of generating such interfaces automatically. One of our goals in this effort is to provide formal semantics for this and other interoperability efforts. Without such formal semantics, integration of distinct simulation tools requires a non-trivial software development effort that must resolve individual assumptions and differences of distinct models. The purpose of the recently proposed FMI standard [19] is to streamline and simplify such efforts through generation of uniform C code. Unifying semantics of distinct models would support automatic generation of such FMI interfaces.

Model-to-model conversion is an effective method for achieving interoperability between different modeling languages. The conversion between the bond graph and linear graph models has been studied in the 70's. Ort and Martens proposed a topological procedure for converting the bond graph to the linear graph by identifying the correspondence of bonds in a bond graph and edges of a linear graph [20]. While theoretically not every bond graph has a corresponding linear graph [21], Birkett gave a deterministic cut-and-paste method for converting any physical bond graph to the corresponding linear graph model [22]. Bond graphs can also be converted to equivalent models in Simulink or Modelica. Specifically, [23] used bond graphs through Simulink to analyze dynamic systems by transforming bond graphs to equivalent block diagrams; researchers in [24] observed that translating non-causal bond graph models to Modelica is in principle a straightforward process, even if causal assignment cannot be specified in Modelica. The reverse conversion from Modelica to bond graphs has been studied in [25]. Strictly speaking, not every Modelica model can be translated into a bond graph, because power continuity (the energy balance) is strictly enforced by the junction structure of bond graph but does not have to be enforced by interconnection of components in Modelica [26]. Similarly, not all Simulink models may be translated into Modelica models, but translation of selective Simulink models to equivalent Modelica models was considered in [27]. Our goal is to identify a subset of physical models that is supported by all of these languages and provide unified semantics that would remove any ambiguities in such conversions and other interoperability tasks.

[1] Such correspondence may take a form of direct translation or using APIs.

© 2019 by ASME

3 ALGEBRAIC TOPOLOGICAL MODELS OF LUMPED PARAMETER SYSTEMS

3.1 Lumped parameter models as cochains

In algebraic topological view of physics, physical properties are distributed in spacetime over finite chunks of space called p-cells, $(p = 0, 1, 2...)$ that fit together to form a cell complex that decomposes the undelying physical space [28]. All cells are endowed with orientation, or sense of direction, which becomes important in order to properly assign signs to physical properties associated with cells.

All lumped parameter models can be formulated by using 2-dimensional cells complexes: 0-cells (nodes), 1-cells (edges), and 2-cells (cycles or "meshes"). These complexes are abstract in the sense that geometric coordinates or shapes of the cells are immaterial; only their connectivity carries important physical information.[2] The distribution of physical properties is described by assigning their types and quantities to the individual cells in this complex. The formal mechanism for doing so requires discretizing the property g over p-cells e^p_α as a *p-cochain* C^p, a formal sum $C^p = \sum_{\alpha=1}^{n_p} g_\alpha e^p_\alpha$.

The relation between physical properties is governed by two types of fundamental laws: metric laws and topological laws. Metric laws usually involve measurement while topological laws relate physical properties associated with space and its boundary. Topological laws can be formulated using formal linear coboundary δ operations on cochains. Specifically, coboundary δ_p operating on a p-cochain produces a $(p+1)$-cochain by transferring and adding the coefficient of the p-cochain to its cofaces (Eq.1). Formally,

$$\delta_p(C^p) = \delta_p\left(\sum_{\alpha=1}^{n_p} g_\alpha e^p_\alpha\right) = \sum_{\beta=1}^{n_{p+1}}\left(\sum_{\alpha=1}^{n_p} h_{\alpha\beta}\cdot g_\alpha\right)\cdot e^{p+1}_\beta \qquad (1)$$

where n_p represents the number of cells in the p-cochain. The incidence coefficient $h_{\alpha\beta} = [e^p_\alpha, e^{p+1}_\beta] \in \{0, \pm 1\}$ is determined by relative orientation of p-cell e^p_α and it cofaces $(p+1)$-cell e^{p+1}_β [10]. If e^{p+1}_β is not a coface of e^p_α, then $h_{\alpha\beta} = 0$; otherwise, if the orientations of e^p_α and e^{p+1}_β are consistent, then $h_{\alpha\beta} = +1$, otherwise, $h_{\alpha\beta} = -1$. If we denote the usual p-incidence matrix as $\mathbf{A} = \left[h_{\beta\alpha}\right]$, then the coboundary operator δ_p is commonly represented by its transpose $\mathbf{A}^T$.

3.2 Physical theories as Tonti diagrams

Every physical theory is conceptualized in terms of relationships between two types of dual physical quantities that are referred to by various authors as configuration/source [10], through/across [12], or effort/flow [6]. In what follows we will adopt Tonti's convention and distinguish between configuration type variables, that are modeled as cochains on primary cell complex decomposition of space, and source variables that are modeled as cochains on the dual cell complex decomposition of the same space.

Physical laws (topological and metric) relate different types of variables within each physical theory. Tonti proposed a systematic method for representing these laws using a diagram that can be considered an evolved combination of the so-called Roth diagrams [29] in terms of cochain sequences and "Maxwell house" diagram to represent all topological and metric relationships in electromagnetism [30]. A simple example of such a diagram is the Tonti diagram of static electrical network theory shown in (Figure 1). It describes the network systems that satisfy Kirchhoff Current Law (KCL) and Kirchhoff Voltage Law (KVL) using a pair of cochains complexes dual to each other.

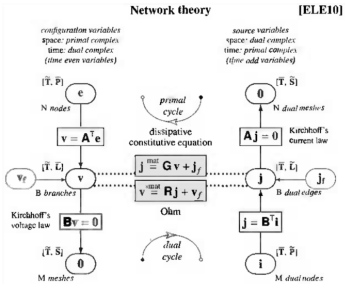

FIGURE 1: Tonti Diagram of network theory - constitutive equations are modified to account for voltage and current sources

The diagram consists of two vertical sequences corresponding to the primal (left) and dual (right) cochain complexes, ordered by dimension. The vertical arrows correspond to the coboundary operations, going down for primal cochains and going up for dual cochains. Formally, the two sequences are exact (the cochain sequence is exact if it satisfies $\delta_p \circ \delta_{p-1} = 0\,(p \geq 1)$) and form two dual cochain complexes:

$$\begin{aligned} \text{primal}: \ & \mathbf{e}^0 \xrightarrow{\delta_0} \mathbf{v}^1 \xrightarrow{\delta_1} \mathbf{0}^2 \\ \text{dual}: \ & \mathbf{0}^2 \xleftarrow{\widetilde{\delta}_1} \mathbf{j}^1 \xleftarrow{\widetilde{\delta}_0} \mathbf{i}^0 \end{aligned} \qquad (2)$$

The measured relationships between dual quantities are represented by the horizontal links in the diagram. In the case of network theory shown in Figure 1, the primal variable are node potentials **e** associated with 0-cells, voltage drops **v** and sources associated with 1-cells, and voltage drops associated with 2-cells

[2] This is in stark contrast to spatially distributed physical phenomena governed by partial differential equation where geometry of cells becomes critical.

© 2019 by ASME

(meshes or cycles) that are identically $\mathbf{0}$ as the consequence of KVL. The cochains of adjacent dimensions satisfy topological laws expressed by the corresponding coboundary operations depicted as down-facing vertical arrows. Thus, 1-cochain of voltage drops $\mathbf{v}^1 = \mathbf{A}^T\mathbf{e}^0$ is implied by the coboundary operation δ_0 on 0-cochain of node potentials $\mathbf{e}^0$; and KVL is just a restatement of the Poincaré lemma. Similarly, the dual source (current) variables: 0-cochain $\mathbf{i}$, 1-cochains $\mathbf{j}$, and 2-cochain $\mathbf{0}$ are indicated in the right branch of the diagram, related by the sequence of two coboundary operations, indicated as arrows going up and expressing KCL.

The reader will notice that the configuration and source variables in Figure 1 are associated with time elements: primal time element for source variables and dual time element for configuration variables. This distinction becomes critical in dynamic physical models [10]. For each type of spatial variable, we can also consider its behavior in time which is represented by a pair of dual 1-dimensional time complexes by respectively using 0-cells $\overline{I}$ and 1-cells $\overline{T}$ to represent primal time instances and intervals and 0-cells $\widetilde{I}$ and 1-cells $\widetilde{T}$ to respectively represent the dual time.

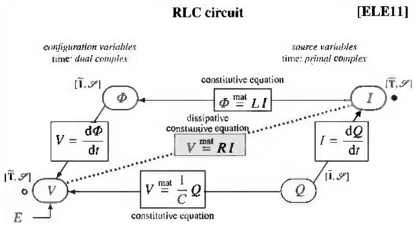

FIGURE 2: Tonti diagram of RLC circuit - only voltage sources are included

The introduction of cell complexes in time has two consequences. First, it identifies the usual time derivative with the corresponding coboundary operator δ^t. Secondly, all space Tonti diagrams now acquire an additional time dimension, giving rise to horizontal sections of the diagram. One such section is shown in Figure 2, which corresponds to the Tonti diagram of RLC circuit systems [10]. Two new constitutive equations describe the capacitance relation between electric charge Q and voltage drop v and the inductance relation between magnetic flow Φ and currents j. Finally, we note that the vertical space diagram in Figure 1 and the horizontal time diagram in Figure 2 can be combined into a single three-dimensional diagram, as described in Section 4 and shown in Figure 4a. In addition to physical quantities in Figure 1 and 2, the diagram in Figure 4a includes magnetic flux potential Ψ and mesh electric charge q that are related by coboundary operators to magnetic flux Φ and electric charge Q respectively. In other words, the extended Tonti diagram includes two additional cochain complexes defined by the two sequences:

$$\begin{aligned} \text{primal}: \ & \mathbf{\Psi}^0 \xrightarrow{\delta_0} \mathbf{\Phi}^1 \xrightarrow{\delta_1} \mathbf{0}^2 \\ \text{dual}: \ & \mathbf{0}^2 \xleftarrow{\widetilde{\delta}_1} \mathbf{Q}^1 \xleftarrow{\widetilde{\delta}_0} \mathbf{q}^0 \end{aligned} \tag{3}$$

3.3 Dual cochain complexes on a single cell complex

In lumped parameter models, dual discretizations are particularly counter-intuitive, since all spatially distributed properties have already been integrated (lumped) and only connectivity of the underlying cell complex remains visible. That connectivity often directly corresponds to the physical embedding; for example, a single electrical network carries both voltage and current information. Similarly, general network model is a single cell complex where primal and dual cochains are represented. The mapping of dual cochains on the primal cell complex is straightforward and is accomplished by mapping the dual $(n-p)$-cells to their corresponding primal p-cells, as shown in Figure 3.

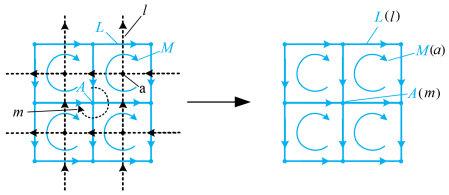

FIGURE 3: Dual cochain complexes on a single cell complex

With this mapping, all $(n-p)$-coboundary operations in dual cell complexes would become the p-boundary operations ∂ in the primal cochain complex, which operate on a p-cochains and produce a $(p-1)$-cochains:

$$\partial_p(C^p) = \partial_p\Big(\sum_{\alpha=1}^{n_p} g_\alpha e_\alpha^p\Big) = \sum_{\beta=1}^{n_{p-1}} \left(\sum_{\alpha=1}^{n_p} h_{\alpha\beta}\cdot g_\alpha\right)\cdot e_\beta^{p-1} \tag{4}$$

which is similar to Eq.1, except that the coefficients are transferred from p-cells to their $(p-1)$-faces. This implies that the coboundary operation $\widetilde{\delta}_{n-p}$ on the dual cells complex is mapped into the boundary operation ∂_p on the primal cell complex,[3] i.e.,

$$\partial_p = \widetilde{\delta}_{n-p} \tag{5}$$

The single complex network model is summarized by a new type of Tonti diagram shown in Figure 4b. Here the dual (source)

[3]This observation also justifies use of ∂_p operator, usually reserved for p-chains, on p-cochains

© 2019 by ASME

cochains have been mapped to the corresponding cochains on the primal cell complex to form the dual cochain complex with boundary ∂_p operators replacing the original dual $\widetilde{\delta}_{n-p}$ coboundary operators. In other words, the dual cochain sequences in (2) and (3) become respectively

$$\begin{aligned} \mathbf{i}^2 &\xrightarrow{\partial_2} \mathbf{j}^1 \xrightarrow{\partial_1} \mathbf{0}^0 \\ \mathbf{q}^2 &\xrightarrow{\partial_2} \mathbf{Q}^1 \xrightarrow{\partial_1} \mathbf{0}^0 \end{aligned} \tag{6}$$

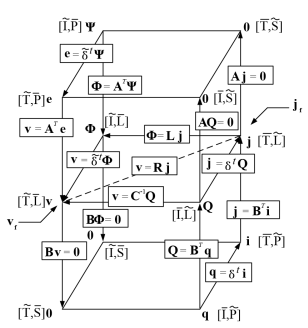

(a) Matrix operators on dual cell complexes

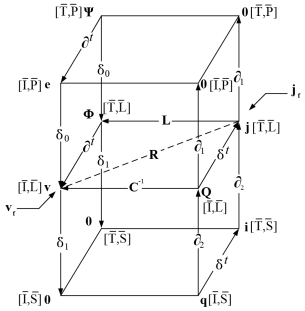

(b) Topological and constitutive relationships on a single cell complex

FIGURE 4: Extended Tonti diagram for RLC network system - with voltage and current sources

In the rest of the paper, we will assume that an algebraic topological model of a lumped parameter system is described by such single (primal) cell complex and a corresponding Tonti diagram with four cochain complexes (corresponding to the four vertical "legs" of the diagram) and all relationships between them.[4]

4 SINGLE-DOMAIN LUMPED PARAMETER SYSTEMS

In this section, we will show how to use Tonti diagrams to describe lumped parameter systems and introduce an automated method of generating system state equations. We will focus on lumped parameter models of a single physical domain, exemplified by classical RLC electrical circuit systems. Application to other physical domains is immediate, since all such models are isomorphic.

Classical single-domain RLC electrical circuits consist of five types of physical elements: resistors, capacitors, inductors, voltage sources and current sources. The algebraic topological structure of dynamic electrical circuits relies on cochains from all four cochain complexes modeled over a single cell complex. The topological and constitutive relations between these cochains are given by the diagram in Figure 4b and one method[5] of generating the state equations is indicated by paths in the diagrams shown in Figure 5. Each path is a sequence of the arrows indicating composition of the corresponding physical laws. The middle horizontal section of the diagram allows three alternative (pink, purple and blue) paths relating the primal 1-cochain of voltage drops $\mathbf{v}^1$ and the dual 1-cochain of branch currents $\mathbf{j}^1$ corresponding to capacitance, resistance, and inductance constitutive relationship respectively. The presence of alternative paths indicate superposition of the corresponding equations generated by each path.

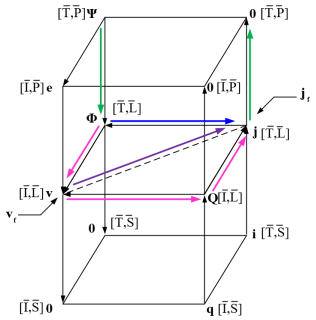

FIGURE 5: State equation generation paths on the extended Tonti diagram with the selected state variable: $\mathbf{\Psi}^0$

The paths in Figure 5 select 0-cochain $\mathbf{\Psi}^0$ as the state variable. The system state equation can be generated by composition of five physical laws (two topological and three constitutive) starting with a 0-cochain $\mathbf{\Psi}^0$. First, coboundary operator in space δ_0 applied to potential magnetic fluxes $\mathbf{\Psi}^0$ in order to generate magnetic fluxes $\mathbf{\Phi}^1$. Now the path splits in two: the blue arrow corresponds to constitutive law $\mathbf{L}^{-1}$ (of the inductor) that relates the magnetic fluxes to branch currents of inductors; the pink arrow takes the magnetic fluxes to generate voltage drops $\mathbf{v}^1$ via the boundary operator in time ∂_1^t. From here the path splits in two again: the purple arrow corresponds to the constitutive Ohm's law $\mathbf{G}$ that relates the voltage drops to branch currents of resistors; continuing along the pink path, the constitutive capacitance law $\mathbf{C}$ relates the voltage drops to electric charges $\mathbf{Q}^1$ of capacitors is followed by the time coboundary operator δ_0^t applied to electric charges of capacitors to generate branch currents of capacitors. Note that the three paths corresponding to the three

[4] Strictly speaking, using ∂_p operators give rise to chain complexes, but it should be clear that these chain complexes on the primal cell complex are isomorphic to the cochain complexes over the dual cell complex.

[5] Other methods to generate the state equations refer to our technical report [31]

© 2019 by ASME

constitutive laws merge into a single 1-cochain of branch currents $\mathbf{j}^1$, which is then transformed one more time by the upward green arrow corresponding to KCL $\partial_1 \mathbf{j}^1 = \mathbf{0}$. Taking into account the voltage and current sources and collecting them to the right hand side of the equation, above processes results in state equations Eq.7.

$$\partial_1 \left(\underbrace{\delta_0^t \mathbf{C} \partial_1^t \delta_0 \mathbf{\Psi}^0}_{\text{currents of C}} + \underbrace{\mathbf{R}^{-1} \partial_1^t \delta_0 \mathbf{\Psi}^0}_{\text{currents of R}} + \underbrace{\mathbf{L}^{-1} \delta_0 \mathbf{\Psi}^0}_{\text{currents of L}} \right) = \partial_1 \left[\underbrace{\mathbf{j}_\mathbf{f}^1}_{\text{current sources}} \quad \underbrace{- \left(\delta_0^t \mathbf{C} + \mathbf{R}^{-1} + \mathbf{L}^{-1} \delta_0^t \right) \mathbf{v}_\mathbf{f}^1}_{\substack{\text{equivalent current sources} \\ \text{generated from} \\ \text{voltage sources}}} \right] \tag{7}$$

In lumped parameter systems, space and time are treated separately, and discretization of time is often delayed until a particular numerical integration scheme is chosen. In this case, viewing boundary ∂_1^t and coboundary δ_0^t operations as differentiation in time syntactically transforms Eq.7 to a more familiar form:

$$\partial_1 \left(\underbrace{\mathbf{C} \delta_0 \ddot{\mathbf{\Psi}}^0}_{\text{currents of C}} + \underbrace{\mathbf{R}^{-1} \delta_0 \dot{\mathbf{\Psi}}^0}_{\text{currents of R}} + \underbrace{\mathbf{L}^{-1} \delta_0 \mathbf{\Psi}^0}_{\text{currents of L}} \right) = \partial_1 \left[\underbrace{\mathbf{j}_\mathbf{f}^1}_{\text{current sources}} \quad \underbrace{- \left(\mathbf{C} \dot{\mathbf{v}}_\mathbf{f}^1 + \mathbf{R}^{-1} \mathbf{v}_\mathbf{f}^1 + \mathbf{L}^{-1} \int \mathbf{v}_\mathbf{f}^1 dt \right)}_{\substack{\text{equivalent current sources} \\ \text{generated from} \\ \text{voltage sources}}} \right] \tag{8}$$

5 MULTI-DOMAIN LUMPED PARAMETER SYSTEMS

5.1 Interactions of single-domain models

Engineering systems are usually constructed as compositions of single-domain subsystems in order to perform complex engineering tasks. We will refer to such systems as multi-domain systems, where lumped-parameter behavior of each single-domain is governed by an extended Tonti diagram as described in the previous section. Composition of two single-domain systems is associated with the process of energy conversion between the two systems, also called *transduction* [6]. Devices used to couple the same type variables of different physical domains are usually called transformers, while devices coupling the dual type variables are called gyrators. Transformers and gyrators with no energy loss are called ideal transformers and gyrators [6].

In our proposed combinatorial model of lumped parameter systems, physical transducer devices can be abstracted by additional relations between primal and dual variables in each of the subsystems; such relations may be governed by additional constitutive, interaction, or conservation constrains imposed on the multi-domain system [32]. In principle, such a representation is sufficient for capturing the behavior of a multi-domain system. Each Tonti diagram corresponds to a system of ordinary differential equations that are coupled by the transducer constraints. However, this representation neither recognizes nor takes advantage of the fact that all single-domain behaviors are isomorphic, which allows to treat the whole multi-domain system as a collection of four constrained cochain complexes on a *single* cell complex model. Below we will define such a model, which takes a form of a generalized Tonti diagram. We then show that, in the presence of two most common transducers: ideal transformers and gyrators, the governing equations for such a model may be generated by following the paths on the generalized Tonti diagram. This results extends the result of Section 4 to multi-domain lumped parameter systems.

5.2 Generalized Tonti diagram for multi-domain systems

Since lumped parameter models in different physical domain are isomorphic, so are their corresponding Tonti diagrams. In this sense, a single Tonti diagram describes behavior of all lumped parameter systems, provided that the variable of the same space-time type are identified and generalized. Two most common generalizations are mechanical (generalized displacement-force model) and electrical (generalized voltage-current model). For the sake of consistency with the discussion in Section 4, we will adopt the generalized electrical model. For example, the electrical resistors, mechanical dampers and hydraulic resistors are all identified as generalized resistors, and so on. In order to emphasize the generalized nature of all physical quantities and to distinguish them from the actual physical electrical network model, we will choose a different set of symbols. Specifically, the generalized Tonti diagram is defined by four exact cochain sequences on a single cell complex:

$$\text{primal}: \quad \mathbf{p}^0 \xrightarrow{\delta_0} \mathbf{a}^1 \xrightarrow{\delta_1} \mathbf{0}^2 \tag{9}$$

$$\mathbf{d}^0 \xrightarrow{\delta_0} \mathbf{u}^1 \xrightarrow{\delta_1} \mathbf{0}^2 \tag{10}$$

$$\text{dual}: \quad \mathbf{s}^2 \xrightarrow{\partial_2} \mathbf{t}^1 \xrightarrow{\partial_1} \mathbf{0}^0 \tag{11}$$

$$\mathbf{n}^2 \xrightarrow{\partial_2} \mathbf{m}^1 \xrightarrow{\partial_1} \mathbf{0}^0 \tag{12}$$

© 2019 by ASME

,where $\mathbf{p}^0$ is a 0-cochain generalized potentials, $\mathbf{a}^1$ is a 1-cochain generalized voltages, $\mathbf{d}^0$ is a 0-cochain generalized potential magnetic fluxes, $\mathbf{u}^1$ is a 1-cochain generalized magnetic fluxes, $\mathbf{s}^2$ is a 2-cochain generalized mesh currents, $\mathbf{t}^1$ is a 1-cochain generalized currents, $\mathbf{n}^2$ is 2-cochain generalized mesh charges, and $\mathbf{m}^1$ is a 1-cochain generalized electric charges. There are also four cochains that are always $\mathbf{0}$: 2-cochain of generalized mesh magnetic fluxes, 2-cochain of generalized mesh voltages, 0-cochain of generalized node currents and 0-cochain of generalized node electric charges.

With such a generalization, all the physical variables of the same space-time type are replaced by their generalized counterparts, effectively transforming model of the heterogeneous multi-domain system in an abstract (generalized) homogeneous system. The behavior of this system is governed by the generalized Tonti diagram shown in Figure 6. As before, the generalized primal and dual cochains are related by (generalized) constitutive relations: resistance $\mathbf{R}_g$, capacitance $\mathbf{C}_g$, and inductance $\mathbf{L}_g$.

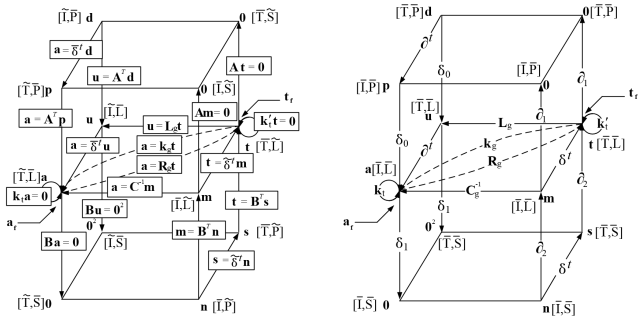

(a) Matrix operators on dual cell complexes (b) Topological operators on a single cell complex

FIGURE 6: Generalized extended Tonti diagram for generalized RLC network system

Furthermore, since all physical quantities are generalized, the actions of ideal transformers and gyrators can be modeled simply as additional constraints on the cochains in the generalized Tonti diagram. Traditionally, a transformer is abstracted as a linear transformation

$$\begin{cases} \begin{bmatrix} 1 & -k_t \end{bmatrix} \cdot \begin{bmatrix} a_1 & a_2 \end{bmatrix}^T = 0 \\ \begin{bmatrix} 1 & -k_t^{-1} \end{bmatrix} \cdot \begin{bmatrix} t_1 & t_2 \end{bmatrix}^T = 0 \end{cases} \tag{13}$$

,where k_t is the transformer's modulus measuring the ratio between two (generalized) voltages a_1 and a_2, as well as the reciprocal ratio between the generalized currents t_1 and t_2 in order to enforce energy balance $a_1 t_1 = a_2 t_2$. Generalizing, every ideal transformer can be represented by a pair of linear constraints $\mathbf{k}_t \mathbf{a} = 0$ and $\mathbf{k}_t' \mathbf{t} = 0$ on cochains of generalized voltages $\mathbf{a}$ and currents $\mathbf{t}$. These constraints are indicated on the generalized Tonti diagram in Figure 6 by two cycles. Similarly, the effect of an abstract gyrator is usually described by a linear transformation

$$\begin{bmatrix} a_1 \\ a_2 \end{bmatrix} = \begin{bmatrix} 0 & k_g \\ k_g & 0 \end{bmatrix} \begin{bmatrix} t_1 \\ t_2 \end{bmatrix} \tag{14}$$

,where the modulus k_g relates the dual quantities in two interacting domains: generalized voltage a_1 of the first domain is proportional to the generalized current t_2 of the second domain, and vice versa, again satisfying the ideal energy balance law. Equivalently, a generalized gyrator may be represented by a linear transformation $\mathbf{k}_g$ that relates the cochains of generalized voltages and currents, as indicated by a dotted arrow in the Tonti diagram in Figure 6.

5.3 System state equations of multi-domain systems

With all physical variables generalized, the heterogeneous multi-domain system now becomes a homogeneous multi-domain system in terms of generalized physical variables. Instead of multiple 2-cochain complexes associated with different types of physical variables, the algebraic topological model of the multi-domain system is now a set of 2-cochain complexes associated with the same (generalized) type of physical variables that are defined over a single cell complex and are constrained by abstract transformers and gyrators.

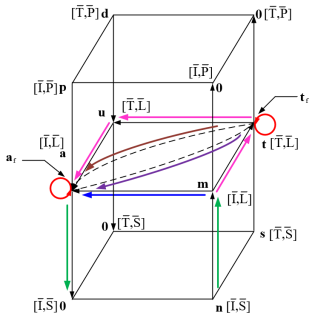

FIGURE 7: State equation generation paths on the generalized extended Tonti diagram with the selected state variable: $\mathbf{n}^2$

One method[6] of generating the state equations is indicated by paths in the generalized Tonti diagram shown in Figure 7. The paths select the 2-cochain $\mathbf{n}^2$ as the state variable. The system

[6]Other methods to generate the state equations refer to our technical report [31]

© 2019 by ASME

state equation can be generated by composition of seven physical laws (two topological and five constitutive) starting with a 2-cochain $\mathbf{n}^2$. First, boundary operator in space ∂_2 applied to generalized mesh electric charge $\mathbf{n}^2$ in order to generate generalized electric charge $\mathbf{m}^1$. Now the path splits into two: the blue arrow corresponds to constitutive law $\mathbf{C}_g^{-1}$ that relates generalized electric charge to generalized voltages of generalized capacitors; the pink arrow takes the generalized electric charge to generate generalized current $\mathbf{t}^1$ via the coboundary operator in time δ_0^t. From here the path splits into four: (1) the purple arrow corresponds to the constitutive law $\mathbf{R}_g$ that relates generalized currents to generalized voltages of generalized resistors; (2) the brown arrow corresponds to the constitutive law $\mathbf{k}_g$ that relates generalized currents to generalized voltages of gyrators; (3) the red cyclic arrow on the right corresponds to constitutive law $\mathbf{k}_t'$ that constrains the generalized currents of generalized transformers; (4) the pink arrow takes the generalized currents to generate generalized magnetic fluxes of generalized inductors by using constitutive law $\mathbf{L}_g$, followed by taking the generalized magnetic fluxes to generate generalized voltages of generalized inductors via the boundary operator in time ∂_1^t. Note that these four paths and the left red cyclic path corresponding to five constitutive laws merge into a single 1-cochain of generalized voltages $\mathbf{a}^1$, which is then transformed one more time by the downward green arrow corresponding to KCL $\delta_1\mathbf{a}^1 = \mathbf{0}$. Taking into account the generalized sources, collecting the terms with known generalized sources and moving them to the right hand side, and interpreting boundary ∂_1^t and coboundary δ_0^t operations as differentiation in time, above procedure results in the state equation[7] Eq.15, with $\mathbf{k}_t'\left(\delta_0^t\partial_2\mathbf{n}^2 - \mathbf{t}_\mathrm{f}^1\right) = \mathbf{0}$ and $\mathbf{k}_\mathrm{t}\left(\mathbf{a}^1 - \mathbf{a}_\mathrm{f}^1\right) = \mathbf{0}$ being the constraint equations.

$$\delta_1\left(\underbrace{\mathbf{L}_g\partial_2\ddot{\mathbf{n}}^2}_{\substack{\text{generalized voltages}\\ \text{of generalized L}}} + \underbrace{\mathbf{R}_g\partial_2\dot{\mathbf{n}}^2}_{\substack{\text{generalized voltages}\\ \text{of generalized R}}} + \underbrace{\mathbf{C}_g^{-1}\partial_2\mathbf{n}^2}_{\substack{\text{generalized voltages}\\ \text{of generalized C}}} + \underbrace{\mathbf{k}_g\partial_2\dot{\mathbf{n}}^2}_{\substack{\text{generalized voltages}\\ \text{of gyrators}}} + \underbrace{\mathbf{a}_T^1}_{\substack{\text{generalized voltages}\\ \text{of transformers}}}\right)$$
$$= \delta_1\left(\underbrace{-\mathbf{a}_\mathbf{f}^1}_{\substack{\text{generalized voltages}\\ \text{sources}}} \underbrace{+\mathbf{L}_g\dot{\mathbf{t}}_\mathbf{f}^1 + \mathbf{R}_g\mathbf{t}_\mathbf{f}^1 + \mathbf{k}_g\mathbf{t}_\mathbf{f}^1 + \mathbf{C}_g^{-1}\int\mathbf{t}_\mathbf{f}^1 dt}_{\substack{\text{equivalent generalized voltage}\\ \text{sources generated from}\\ \text{generalized current sources}}}\right) \tag{15}$$

Example 1. *We will use an example of multi-domain electrical-mechanical system in Figure 8a to illustrate the derivation of Eq.15. The shown electrical-mechanical system contains two resistors R_1, R_2, one capacitor C_1, one inductor L_1, one voltage source V_s, one moment of inertia J, one external torque τ, one electrical transformer and one DC motor. The transformer between two electrical domains is an ideal electrical transformer with turns ratio N_1/N_2; the gyrator between the electrical and the mechanical domain is an ideal DC motor, where the ratio of the voltage drop and the rotational velocity is k_g. Topologically, the system is a 2-cell complex shown in Figure 8b, and consisted of nine 0-cells P_i $(i = 1 \sim 9)$, nine 1-cells (L_{R_1},L_{C_1},L_{TL},L_{TR}, L_{R_2},L_{L_1}, L_{GL},L_{GR},L_J) and three 2-cells (M_1,M_2,M_3). We use symbol -TF- to represent the abstract transformer and a symbol -GY- to represent the abstract gyrator. These two symbols identify the cells where the energy transaction may occur.*

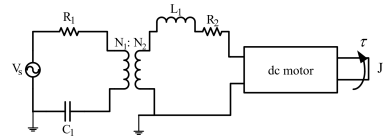

(a) A multi-domain electro-mechanical system

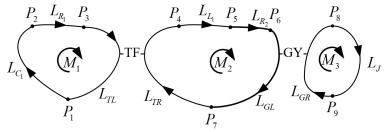

(b) Topological structure

FIGURE 8: An electro-mechanical system and its topological structure

[7] Note that the generalized voltages of transformers $\mathbf{a}_T^1$ cannot be directly obtained from the generalized currents of transformers $\mathbf{t}_T^1$, so we treat them as additional unknown variables in the system state equation.

© 2019 by ASME

The algebraic topological model of the system contians: primal 0-cochain generalized potential magnetic fluxes ($\mathbf{d}^0 = d_1 \cdot P_1 + d_2 \cdot P_2 + d_3 \cdot P_3 + d_4 \cdot P_4 + d_5 \cdot P_5 + d_6 \cdot P_6 + d_7 \cdot P_7 + d_8 \cdot P_8 + d_9 \cdot P_9$), primal 0-cochain generalized potentials ($\mathbf{p}^0 = p_1 \cdot P_1 + p_2 \cdot P_2 + p_3 \cdot P_3 + p_4 \cdot P_4 + p_5 \cdot P_5 + p_6 \cdot P_6 + p_7 \cdot P_7 + p_8 \cdot P_8 + p_9 \cdot P_9$), primal 1-cochain generalized magnetic fluxes ($\mathbf{u}^1 = u_1 \cdot L_{R_1} + u_2 \cdot L_{C_1} + u_3 \cdot L_{TL} + u_4 \cdot L_{TR} + u_5 \cdot L_{R_2} + u_6 \cdot L_{L_1} + u_7 \cdot L_{GL} + u_8 \cdot L_{GR} + u_9 \cdot L_J$), primal 1-cochain generalized voltages ($\mathbf{a}^1 = a_1 \cdot L_{R_1} + a_2 \cdot L_{C_1} + a_{TL} \cdot L_{TL} + a_{TR} \cdot L_{TR} + a_5 \cdot L_{R_2} + a_6 \cdot L_{L_1} + a_{GL} \cdot L_{GL} + a_{GR} \cdot L_{GR} + a_9 \cdot L_J$), dual 1-cochain generalized currents ($\mathbf{t}^1 = t_1 \cdot L_{R_1} + t_2 \cdot L_{C_1} + t_{TL} \cdot L_{TL} + t_{TR} \cdot L_{TR} + t_5 \cdot L_{R_2} + t_6 \cdot L_{L_1} + t_{GL} \cdot L_{GL} + t_{GR} \cdot L_{GR} + t_9 \cdot L_J$), dual 1-cochain generalized electric charges ($\mathbf{m}^1 = m_1 \cdot L_{R_1} + m_2 \cdot L_{C_1} + m_{TL} \cdot L_{TL} + m_{TR} \cdot L_{TR} + m_5 \cdot L_{R_2} + m_6 \cdot L_{L_1} + m_{GL} \cdot L_{GL} + m_{GR} \cdot L_{GR} + m_9 \cdot L_J$), dual 2-cochain generalized mesh electric charges $\mathbf{n}^2 = n_1 \cdot M_1 + n_2 \cdot M_2 + n_3 \cdot M_3$, dual 2-cochain generalized mesh currents $\mathbf{s}^2 = s_1 \cdot M_1 + s_2 \cdot M_2 + s_3 \cdot M_3$ and four cochains that are always $\mathbf{0}$: 2-cochain of generalized mesh magnetic fluxes, 2-cochain of generalized mesh voltages, 0-cochain of generalized node currents and 0-cochain of generalized node electric charges. In order to obtain unique solution of the state equations, we consider 0-cells P_1, P_7 and P_9 as the reference node. Following the paths shown in Figure 7, generates the system state equation as follows[8]

$$\begin{cases} \begin{bmatrix} 0 & 0 & 0 \\ 0 & L_{g_1} & 0 \\ 0 & 0 & L_{g_2} \end{bmatrix} \ddot{\mathbf{n}}^2 + \begin{bmatrix} R_{g_1} & 0 & 0 \\ 0 & R_{g_2} & k_g \\ 0 & k_g & 0 \end{bmatrix} \dot{\mathbf{n}}^2 + \begin{bmatrix} C_{g_1}^{-1} & 0 & 0 \\ 0 & 0 & 0 \\ 0 & 0 & 0 \end{bmatrix} \mathbf{n}^2 + \begin{bmatrix} \mathrm{a}_{TL} \\ \mathrm{a}_{TR} \\ 0 \end{bmatrix} = \begin{bmatrix} 0 \\ 0 \\ 0 \end{bmatrix} \\ \mathrm{a}_{TL} / \mathrm{a}_{TL} = N_1 / N_2 \\ \dot{\mathbf{n}}^2_{(1)} \Big/ \dot{\mathbf{n}}^2_{(2)} = N_2 / N_1 \end{cases} \tag{16}$$

6 CONCLUSION AND PROMISING DIRECTIONS

The difference in syntax and semantics of system modeling languages results in many challenges in model exchange, translation, and composition. Standardizing on a semantics of these languages is a key to solving such widespread interoperability challenge that arise with rapid proliferation of model-based engineering language and tools. Moreover, formal semantics of engineering models is also a principal ingredient of rigorous and algorithmic foundations for model-based systems engineering. In this paper, we proposed a formal semantics for a large and important class of lumped-parameter systems that are widely used for systems engineering, physical modeling, and design activities. The proposed semantics relies only on standard tools from algebraic topology and known results in classification of physical theories and systems. The semantics is effectively "representation free" in that it is independent of specific implementation assumptions, coordinates, linguistic constructs, or numerical simulation schemes. We showed that (extended and generalized) Tonti diagrams provide a canonical method for representing behaviors of lumped parameter systems computationally. Based on known classification of physical theories, behavior of any lumped parameter system may be described either as a collection of interacting single-domain Tonti diagrams or as a single generalized Tonti diagram with energy transduction represented by additional constraints. In other words, a Tonti diagram can be viewed as a representation scheme and a data structure for representing most known physical behaviors. We have also seen that this representation supports algorithmic generation of all possible forms of the governing state equations as paths in the (collection of) Tonti diagrams.

Treating the common semantic model and its representation by Tonti diagrams as the first class objects, that explicitly represent physical behaviors, opens up a number of promising and exciting opportunities in computational design and model-based engineering. Algorithmic construction, editing, composition, and transformation of such models would support a broad range of design engineering activities, from concept generation to detailed system modeling. Because many such engineering activities are performed using SysML, it may be reasonable to expect that Tonti diagrams should appear as one of the standard diagrams in SysML in the near future. Such a diagram would provide immediate support for including physical behaviors and their simulation into a broad range of model-based systems engineering activities.

ACKNOWLEDGMENT

This research is supported by the National Institute of Standards and Technology (NIST) under agreement 70NANB14H248, by NSF grants CMMI-1344205, CMMI-1361862, and CMMI-1547189, and by Defense Advanced Research Projects Agency's FUNdamental Design Program. The responsibility for errors and omissions lies solely with the authors.

REFERENCES

[1] Kluever, C. A., 2015. *Dynamic systems: modeling, simulation, and control*. John Wiley & Sons.

[2] Paynter, H. M., 1961. *Analysis and design of engineering systems*. MIT press.

[3] Rowell, D., and Wormley, D. N., 1997. *System dynamics: an introduction*. Prentice Hall.

[4] Elmqvist, H., and Mattsson, S. E., 1997. *An introduction to the physical modeling language Modelica*, Vol. 97.

[5] Chaturvedi, D. K., 2009. *Modeling and simulation of systems using MATLAB and Simulink*. CRC Press.

[8] Refer to our technical report [31] for more detailed procedure of generating this equation

© 2019 by ASME

[6] Karnopp, D. C., Margolis, D. L., and Rosenberg, R. C., 2012. *System dynamics: modeling, simulation, and control of mechatronic systems*. John Wiley & Sons.

[7] Fritzson, P., and Engelson, V., 1998. *Modelica - A unified object-oriented language for system modeling and simulation*. Springer.

[8] Bock, C., Barbau, R., Matei, I., and Dadfarnia, M., 2017. "An extension of the systems modeling language for physical interaction and signal flow simulation". *Systems Engineering,* ***20***(5), pp. 395–431.

[9] Otter, M., 2010. "Functional mockup interface (fmi) for model exchange". *Modelica Newsletter,* ***1***.

[10] Tonti, E., 2013. *The mathematical structure of classical and relativistic physics*. Springer.

[11] Roth, J. P., 1955. "An application of algebraic topology to numerical analysis: On the existence of a solution to the network problem". *Proceedings of the National Academy of Sciences,* ***41***(7), pp. 518–521.

[12] Branin, F. H., 1966. "The algebraic-topological basis for network analogies and the vector calculus". In Symposium on generalized networks, pp. 453–491.

[13] Kron, G., 1963. *Diakoptics: the piecewise solution of large-scale systems*, Vol. 2. MacDonald.

[14] Gomes, C., Thule, C., Broman, D., Larsen, P. G., and Vangheluwe, H., 2017. "Co-simulation: State of the art". *arXiv preprint arXiv:1702.00686*.

[15] Friedenthal, S., Moore, A., and Steiner, R., 2014. *A practical guide to SysML: the systems modeling language*. Morgan Kaufmann.

[16] Sindico, A., Di Natale, M., and Panci, G., 2011. "Integrating sysml with simulink using open-source model transformations.". In SIMULTECH, pp. 45–56.

[17] Johnson, T., Kerzhner, A., Paredis, C. J., and Burkhart, R., 2012. "Integrating models and simulations of continuous dynamics into sysml". *Journal of Computing and Information Science in Engineering,* ***12***(1), p. 011002.

[18] Turki, S., and Soriano, T., 2005. "A sysml extension for bond graphs support". In Proc. of the International Conference on Technology and Automation (ICTA), Greece, Citeseer.

[19] Blochwitz, T., Otter, M., Arnold, M., Bausch, C., Elmqvist, H., Junghanns, A., Mauß, J., Monteiro, M., Neidhold, T., Neumerkel, D., et al., 2011. "The functional mockup interface for tool independent exchange of simulation models". In Proceedings of the 8th International Modelica Conference; March 20th-22nd; Technical Univeristy; Dresden; Germany, no. 063, Linköping University Electronic Press, pp. 105–114.

[20] Ort, J., and Martens, H., 1974. "A topological procedure for converting a bond graph to a linear graph". *Journal of Dynamic Systems, Measurement, and Control,* ***96***(3), pp. 307–314.

[21] Perelson, A. S., and Oster, G. F., 1976. "Bond graphs and linear graphs". *Journal of the Franklin Institute,* ***302***(2), pp. 159–185.

[22] Birkett, S., and Roe, P., 1989. "The mathematical foundations of bond graphs—i. algebraic theory". *Journal of the Franklin Institute,* ***326***(3), pp. 329–350.

[23] Calvo, J. A., Álvarez-Caldas, C., and San Román, J. L., 2011. *Analysis of Dynamic Systems Using Bond Graph Method Through SIMULINK*. INTECH Open Access Publisher.

[24] Broenink, J. F., 1999. "Object-oriented modeling with bond graphs and modelica". *SIMULATION SERIES,* ***31***, pp. 163–168.

[25] D'abreu, M. C., and Wainer, G. A., 2006. "A bond-graph mapping mechanism for m/cd+".

[26] Borutzky, W., 2009. *Bond graph methodology: development and analysis of multidisciplinary dynamic system models*. Springer Science & Business Media.

[27] Dempsey, M., 2003. "Automatic translation of simulink models into modelica using simelica and the advancedblocks library". In Paper presented at the 3rd International Modelica Conference, Citeseer.

[28] Hatcher, A., 2001. "Algebraic topology".

[29] Roth, J. P., 1971. "Existence and uniqueness of solution to electrical network problem via homology sequences". In SIAM-AMS Proceedings, Vol. III, American Mathematical Society, pp. 113–118.

[30] Bossavit, A., 1998. *Computational electromagnetism: variational formulations, complementarity, edge elements*. Academic Press.

[31] Wang, R., and Shapiro, V., 2018. "Topological Semantics for Lumped Parameter Systems Modeling". *arXiv e-prints*, Nov, p. arXiv:1811.02666.

[32] Tonti, E., 2003. A classification diagram for physical variables.

© 2019 by ASME

View publication stats